ELSEVIER

Journal of Alloys and Compounds 408–412 (2006) 693–700

Journal of
ALLOYS
AND COMPOUNDS

www.elsevier.com/locate/jallcom

Photoinduced self-assembly to lanthanide-containing molybdenum-blue superclusters and molecular design

Toshihiro Yamase [a,b,*], Eri Ishikawa [a,b], Yohko Abe [a,b], Yutaka Yano [a,b]

[a] *Chemical Resources Laboratory, Tokyo Institute of Technology, R1-21, 4259 Nagatsuta, Midori-ku, Yokohama 226-8503, Japan*
[b] *Core Research for Evolutional Science and Technology (CREST), Japan Science and Technology Agency (JST),*
4-1-8 Honcho, Kawaguchi 332-0012, Japan

Received 31 July 2004; accepted 25 November 2004
Available online 29 June 2005

Abstract

The prolonged photolysis of aqueous solutions containing $[\mathrm{Mo_{36}O_{112}(H_2O)_{16}}]^{8-}$, $[{}^{i}\mathrm{PrNH_3}]^{+}$ (or $[p\text{-}\mathrm{CH_3C_6H_4SO_2}]^{-}$), and $\mathrm{LaCl_3}$ at $\mathrm{pH} = 1$ leads to the formation of 28-electron reduced $[\mathrm{Mo_{28}{}^{V}Mo_{122}{}^{VI}O_{452}H_2(H_2O)_{66}\{La(H_2O)_5\}_2}]^{24-}$ ($\equiv\{\mathrm{Mo_{150}(La)_2}\}$) or 24-electron reduced $[\mathrm{Mo_{24}{}^{V}Mo_{96}{}^{VI}O_{366}H_{14}(H_2O)_{48}\{La(H_2O)_5\}_6}]^{4-}$ ($\equiv\{\mathrm{Mo_{120}(La)_6}\}$) molybdenum-blue nano-ring which depends on the electron donor species. The former is of the ellipsoidal structure with approximately 35 and 32 Å for the outer ring diameters and 25 and 20 Å for the inner ring diameters. The latter is of the Japanese rice-ball shape with approximately 30 and 17 Å for outer and inner ring diameters, respectively. All the $\mathrm{La^{3+}}$ sites are coordinated into the inner rings with replacement of $[\mathrm{Mo(H_2O)O_2(\mu\text{-}O)Mo(H_2O)O_2}]^{2+}$ ($\equiv\{\mathrm{Mo_2}\}$-*linker*) groups. Each $\mathrm{LaO_9}$ site exhibits the distorted tricapped-trigonal-prismatic geometry which consists of four two-coordinate oxygen atoms from $\{\mathrm{Mo_{150}}\}$ and $\{\mathrm{Mo_{120}}\}$ frameworks and five aqua oxygen atoms, with 2.46–2.62 Å of La–O bond-lengths. The topology of $\{\mathrm{Mo_{150}(La)_2}\}$ and $\{\mathrm{Mo_{120}(La)_6}\}$ structures shows that the $\mathrm{Ln^{3+}}$-incorporated sub-blocks $\{\mathrm{Mo_{10}(La)}\}$and $\{\mathrm{Mo_{11}(La)}\}$ in rings possess large molecular curvature with $\omega_1 \approx 157^\circ$ and $\omega_3 \approx 154^\circ$ compared to $\{\mathrm{Mo_{10}}\}$and $\{\mathrm{Mo_{11}}\}$ with $\omega_1 \approx 158$–159° and $\omega_3 \approx 158^\circ$. Number of the $\{\mathrm{Mo_{10}(La)}\}$and $\{\mathrm{Mo_{11}(La)}\}$ sub-building-blocks in the building-block sequence for the ring is important for both shape and size of nano-rings, which is governed by the manipulation of $\mathrm{Ln^{3+}}$ (with a variety of ionic radius) and electron donors. It is indicated that a variety of the combination of sub-building-blocks with different molecular curvatures among $\{\mathrm{Mo_{10}(La)}\}$, $\{\mathrm{Mo_{11}(La)}\}$, $\{\mathrm{Mo_{10}}\}$, and $\{\mathrm{Mo_{11}}\}$ is a promising method for the molecular design of nano-rings in both the chemical versatility and the functionality.

Keywords: Clusters; Nanostructures; Crystal structure and symmetry; X-ray diffraction

---

1. Introduction

The prolonged photolysis of the $[\mathrm{Mo_7O_{24}}]^{6-}$/electron donor aqueous solution at pH 5–6 results in formation of the dimerically condensed molybdenum-blue, $[(\mathrm{Mo_7O_{23}})_2]^{10-}$ ($\equiv\{\mathrm{Mo_{14}}\}$), which is a *cis*-configurated two-electron reduced species with molecular curvature (consisting of 175° as the central Mo–O–Mo bond angle (ω_1) of the dimer and 157° as the central O–Mo–O bond angle (ω_3) for the half moiety) [1]. On the other hand, the molybdenum-blue species involved in the “classical” thermal reduction of strongly acidified aqueous molybdate solutions have been characterized as much condensed wheel-shaped and spherical anions by Müller, and a variety of combination of molybdates and reducing agents have given both nano-rings such as 28-electron reduced $\{\mathrm{Mo_{142}}\}$ and $\{\mathrm{Mo_{154}}\}$ rings $[\mathrm{Mo_{142}O_{418}(OH)_{14}(H_2O)_{58}}]^{26-}$ and $[\mathrm{Mo_{154}O_{448}(OH)_{14}(H_2O)_{70}}]^{14-}$ and 32-electron reduced $\{\mathrm{Mo_{176}}\}$ ring $[\mathrm{Mo_{176}O_{512}(OH)_{16}(H_2O)_{80}}]^{16-}$ and nano-particles such as 60-electron reduced $\{\mathrm{Mo_{132}}\}$ $[\{\mathrm{Mo_2{}^{V}O_4(CH_3CO_2)}\}_{30}\{\mathrm{(Mo)Mo_5O_{21}(H_2O)_6}\}_{12}]^{12-}$ and $\mathrm{Fe^{3+}}$-containing $\{\mathrm{Mo_{78}Fe_{30}}\}$ $[\mathrm{Mo_{72}Fe_{30}O_{252}(CH_3CO_2)_{12}\{Mo_2O_7(H_2O)\}_2\{H_2Mo_2O_8(H_2O)\}(H_2O)_{91}}]$ [2–5]. We recently showed also that the prolonged photolysis of aqueous

---

[*] Corresponding author. Tel.: +81 45 924 5260; fax: +81 45 924 5260.
E-mail address: tyamase@res.titech.ac.jp (T. Yamase).

0925-8388/$ – see front matter © 2005 Elsevier B.V. All rights reserved.
doi:10.1016/j.jallcom.2004.11.099

solutions containing $[Mo_{36}O_{112}(H_2O)_{16}]^{8-}$ (≡{Mo_{36}}) and alkylammonium cations as electron donors at pH = 1 and 2 leads to the formation of the Müller's nanorings of $[Mo_{28}{}^{V}Mo_{126}{}^{VI}O_{462}(H_2O)_{70}]^{28-}$ (≡{Mo_{154}}) and $[Mo_{28}{}^{V}Mo_{114}{}^{VI}O_{404}(OH)_{28}(H_2O)_{58}]^{12-}$ (≡{Mo_{142}}), respectively [6,7]. The former is an intact car-tire-shaped ring (with D_{7d} symmetry) and the latter is a deficient ring which misses six $[Mo(H_2O)O_2(\mu\text{-}O)Mo(H_2O)O_2]^{2+}$ units (≡{Mo_2}-*linker* units) from the former. Since {Mo_{36}} incorporates two Mo_7O_{24} moieties in its centrosymmetric structure [8], it has been proposed that the photodegradative two-electron reductive condensation of a half molecule ({Mo_{18}}) of {Mo_{36}} proceeds with a mode similar to the {Mo_{14}} formation to yield the $[Mo_{22}O_{70}(H_2O)_{10}]^{12-}$ (≡{Mo_{22}}) building block which undergoes further successive two-electron-photoreductive cyclic heptameric condensations to {Mo_{154}} as a 28-electron reduced species [6,7]. Fig. 1 shows the schemes proposed for the photoinduced self-assembly to {Mo_{154}} through the dehydrative condensations of {Mo_{22}} with similarity to the photodimeric

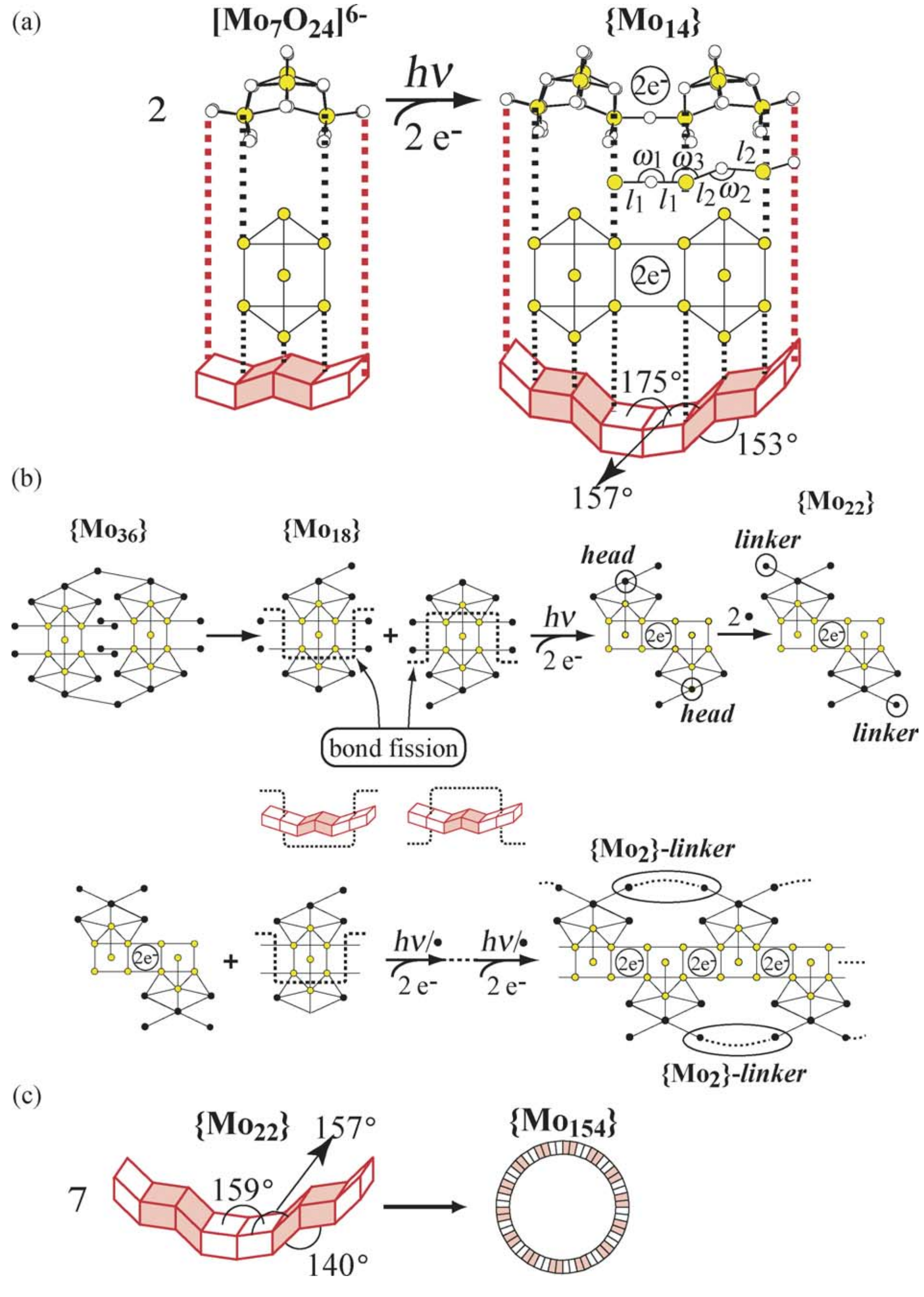

Fig. 1. Schemes proposed for the photoinduced self-assembly to {Mo_{154}} through the dehydrative condensations of {Mo_{22}} with similarity to the photodimeric condensation of $[Mo_7O_{24}]^{6-}$: two-electron reductive condensation of $[Mo_7O_{24}]^{6-}$ to $[(Mo_7O_{23})_2]^{10-}$ ({Mo_{14}}) and their molecular curvatures (a), successive two-electron reductive condensations of {Mo_{36}} to 28-electron reduced {Mo_{154}}(b), and photoreductive cyclic heptamerization of {Mo_{22}} building-blocks to the {Mo_{154}} ring (c).

condensation of $[Mo_7O_{24}]^{6-}$. Each of two inner rings (above and below the equator) of $\{Mo_{154}\}$ consists of seven *head* MoO_6 octahedra and seven $\{Mo_2\}$-*linker* units. $\{Mo_{36}\}$ is a predominant species in aqueous solutions of isopolyoxomolybdates at $pH \leq 2$, thus, acidic conditions at $pH \leq 2$ seems to be essential for the photochemical formation of Mo-blue rings. Furthermore, the photolysis of the $\{Mo_{36}\}$/electron donor system in the presence of trivalent lanthanide cations (with less than one-third of the concentration of $\{Mo_{36}\}$) led to the formation of a nanotube of the intact $\{Mo_{154}\}$ rings, where each inner ring incorporates the di-μ-oxo-linkaged $[MoO_2(\mu\text{-}O)(\mu\text{-}H_2O)MoO_2]^{2+}$ unit instead of one of seven $\{Mo_2\}$-*linker* units [7]. The X-ray crystallographic analysis of the$\{Mo_{154}\}$ nano-tube ($\{[Mo_{28}{}^{V}Mo_{126}{}^{VI}O_{458}H_{12}(H_2O)_{66}]^{8-}\}_{\infty}$) indicates that the Mo–O–Mo linkage motifs of the inner-rings between the neighboring $\{Mo_{154}\}$ rings result from both intermolecular dehydrations between terminal Mo-OH groups of *linkers* and between Mo–H_2O aqua ligand of *linker* and terminal Mo=O groups of *head* (and vice versa), suggesting that the trivalent lanthanide cation (Ln^{3+}) in the vicinity of the inner ring of the $\{Mo_{154}\}$ species acts as a trap of the water molecules liberated on the dehydrated condensation due to its high coordination number (8–12). Since the Ln^{3+}-incorporated nano-rings such as $[Mo_{120}\{Pr(H_2O)_5\}_6O_{366}H_{12}(H_2O)_{48}]^{6-}$ [9] and $[\{Mo_{128}Eu_4O_{388}H_{10}(H_2O)_{81}\}_2]^{20-}$ [10] has been also isolated by Müller and his colleagues, we have investigated the photochemical preparation of the above hypothetical $Ln^{3+}\subset\{Mo_{154}\}$ precursors for the $\{Mo_{154}\}$ tube from the mechanistic standpoint as well as the photochemical design of nanoscopic devices based on the polyoxometalates. In this work the photoinduced self-assemby to La^{3+}-incorporated molybdenum blues of $\{Mo_{150}(La)_2\}$ and $\{Mo_{120}(La)_6\}$ is described and the topology of the formation of these distorted ring structures is discussed based on the photoreductive condensation between the sub-blocks with different molecular curvatures.

2. Experimental

2.1. Synthesis of $[{}^{i}PrNH_3]_{24}[Mo_{28}{}^{V}Mo_{122}{}^{VI}O_{452}H_2(H_2O)_{66}\{La(H_2O)_5\}_2]\cdot 156 \pm 5H_2O$ (*1*)

$(NH_4)_8[Mo_{36}O_{112}(H_2O)_{16}]\cdot 58H_2O$ was synthesized according to the published procedure [8]. ${}^{i}PrNH_2$ (0.35 ml, 4 mmol) with $HClO_4$ acidification (pH 1.0) was added to a solution containing $(NH_4)_8[Mo_{36}O_{112}(H_2O)_{16}]\cdot 58H_2O$ (0.1 g, 0.015 mmol) and $LaCl_3\cdot 7H_2O$ (0.04 g, 0.11 mmol) in 38 ml of H_2O. The resulting solution was irradiated for 2 days using a 500 W superhigh-pressure mercury/xenon lamp. Then, $[{}^{i}PrNH_2]\cdot HClO_4$ (0.6 g, 3.8 mmol) was added to the dark-blue colored photolyte. The rhombohedral dark-blue crystals of **1** were precipitated at room temperature within 2 days. Yield: 0.026 g, 13.8% based on Mo. Calcd. N 1.22%, C 3.14%, H 2.59%; found N 1.30%, C 3.18%, H 1.77%. IR (KBr pellet): ν (cm^{-1}) = 1610 {m, $\delta(H_2O)$}, 972 (m), 910 (w), 749 (s), 633 (s), 558 (s). The manganometric redox titration shows the presence of 28 ± 1 Mo^{V} centers in **1**. Together with the below X-ray crystallographic result, the elemental analysis enables us to formulate **1** as given. The same structural compounds were obtained for Y^{3+}-, Er^{3+}-, and Lu^{3+}-substituted species instead of La^{3+}.

2.2. Synthesis of $[NH_4]_4[Mo_{24}{}^{V}Mo_{96}{}^{VI}O_{366}H_{14}(H_2O)_{48}\{La(H_2O)_5\}_6]\cdot 180 \pm 20H_2O$ (*2*)

$[NH_4]_6[Mo_7O_{24}]\cdot 4H_2O$ (0.12 g, 0.097 mmol) was dissolved in 20 ml of H_2O, and the pH level of the solution was adjusted to 1.2 by HCl. $CH_3C_6H_4SO_2Na\cdot 4H_2O$ (0.058 g, 0.23 mmol) and $LaCl_3\cdot 7H_2O$ (0.04 g, 0.11 mmol) were added into the acidified solution. The solution was exposed to UV light from a 500 W superhigh-pressure mercury/xenon lamp. The deeply blue-colored solution after 2-days irradiation was kept in a Program Incubator Yamato-IN602W programmed by the repeated cycles of (i) 3 h from 20 to 24 °C, (ii) 3h at 24 °C, (iii) 3 h from 24 to 20 °C, and (iv) 3 h at 20 °C, and hexagonal dark-blue crystals were precipitated in a week. The crystals were collected and washed with cold water, thereafter dried under the air. Yield: 58.14 mg, 36.2% based on Mo. Calcd. N 0.24%, H 2.40%; found N 0.22%, H 2.45%. IR (KBr pellet): ν (cm^{-1}) = 1619 {m, $\delta(H_2O)$}, 1384 {m, $\delta(NH_4^+)$}, 973 (m), 910 (w), 744 (s), 640 (s), 559 (s); λ (nm) (ε_M) = 756 (2.6×10^4 l mol^{-1} cm^{-1}), 1044 (3.6×10^4 l mol^{-1} cm^{-1}). The manganometric redox titration shows the presence of 23.1 ± 0.3 Mo^{V} centers in **2**. Together with the below X-ray crystallographic result, the elemental analysis enable us to formulate **2** as given. The same structural compounds were obtained for Ce^{3+}-, Nd^{3+}-, and Sm^{3+}-substituted species instead of La^{3+}.

2.3. Crystal data for *1*

$H_{706}La_2Mo_{150}N_{24}O_{684}C_{72}$, $M = 27524.93$ g mol^{-1}, space group $P2_1/n$, $a = 39.406(10)$ Å, $b = 17.890(4)$ Å, $c = 58.30(2)$ Å, $\beta = 99.074(4)$, $V = 40583.1(17)$ Å^3, $Z = 2$, $\rho = 2.252$ g cm^{-3}, $\mu = 24.34$ cm^{-1}, $F(0\,0\,0) = 26384$. Crystal size = 0.2 mm × 0.2 mm × 0.02 mm. Crystal was coated with paraffin oil and mounted in a loop. Intensity data were measured on a Rigaku/MSC Saturn CCD diffractometer with the graphite monochromatized Mo-Kα radiation (=0.71071 Å) at 113 K. Data collection proceeded using ω-scan at 0.5° scan and $\chi = 45°$ in eight runs (with 360 frames respectively) of $-105.0° < \omega < 75.0°$, $\phi = 0°$; $-105.0° < \omega < 75.0°$, $\phi = 90°$; $-105.0° < \omega < 75.0°$, $\phi = 180°$; $-105.0° < \omega < 75.0°$, $\phi = 270°$. A crystal-to-detector distance was 100.44 mm. The exposure rate was 40.0 s/°. The detector swing angle for the first four runs were 15.17° and for other four runs 38.17°. A total of 353,336 reflections ($0.58° < \theta < 29.57°$) was collected of which 99,390 unique reflections ($R_{int} = 0.065$) were used. Lorentz polarization factor were applied and an empirical absorption correction (multi-scan) using equivalent reflections was performed with the program (ABSCOR; T. Higashi, Program for Absorption Correction, Rigaku Corporation, Tokyo, 1995, and R. Jacobson, private communication, 1998). The structure was solved by direct methods (SHELXS97) and refined (2079 parameters) based on a full-matrix least-squares (on F) by using the CrystalStructure software package (CRYSTALS) to $R = 0.101$ for 25,650 reflections with $I > 4\sigma(I)$, $R_w = 0.126$ for all data: max/min residual electron density 2.61 and $-2.24\,\mathrm{e\,Å^{-3}}$. All the Mo atoms for the anion were refined anisotropically, and all the C, O, and N atoms isotropically. The nineteen crystal-water O atoms (O320–O338) were disordered with half occupancies which were determined based on refinement of their thermal parameters. The positional coordinates of C7, C8, C9, and N3 atoms (which construct ${}^{i}\mathrm{PrNH_3}^{+}$ ammonium) were refined as rigid group. The position of several ${}^{i}\mathrm{PrNH_3}^{+}$ ammoniums and crystal-waters could not be determined due to disorder over all. The calculation of the bond valence sums ($\sum s$) for all the oxygen atoms of La–O and Mo–O bonds indicated the coordination of 76 aqua ligands (for $\sum s < 0.6$) to the anion.

2.4. Crystal data for **2**

$H_{546}Mo_{120}La_6O_{624}N_4$, $M = 22936.2\ \mathrm{g\,mol^{-1}}$, space group $P2_1/c$, $a = 27.805(8)$ Å, $b = 38.764(11)$ Å, $c = 65.55(2)$ Å, $\beta = 99.908(3)^{\circ}$, $V = 69604.5(35)$ Å^3, $Z = 4$, $\rho = 2.189\ \mathrm{g\,cm^{-3}}$,

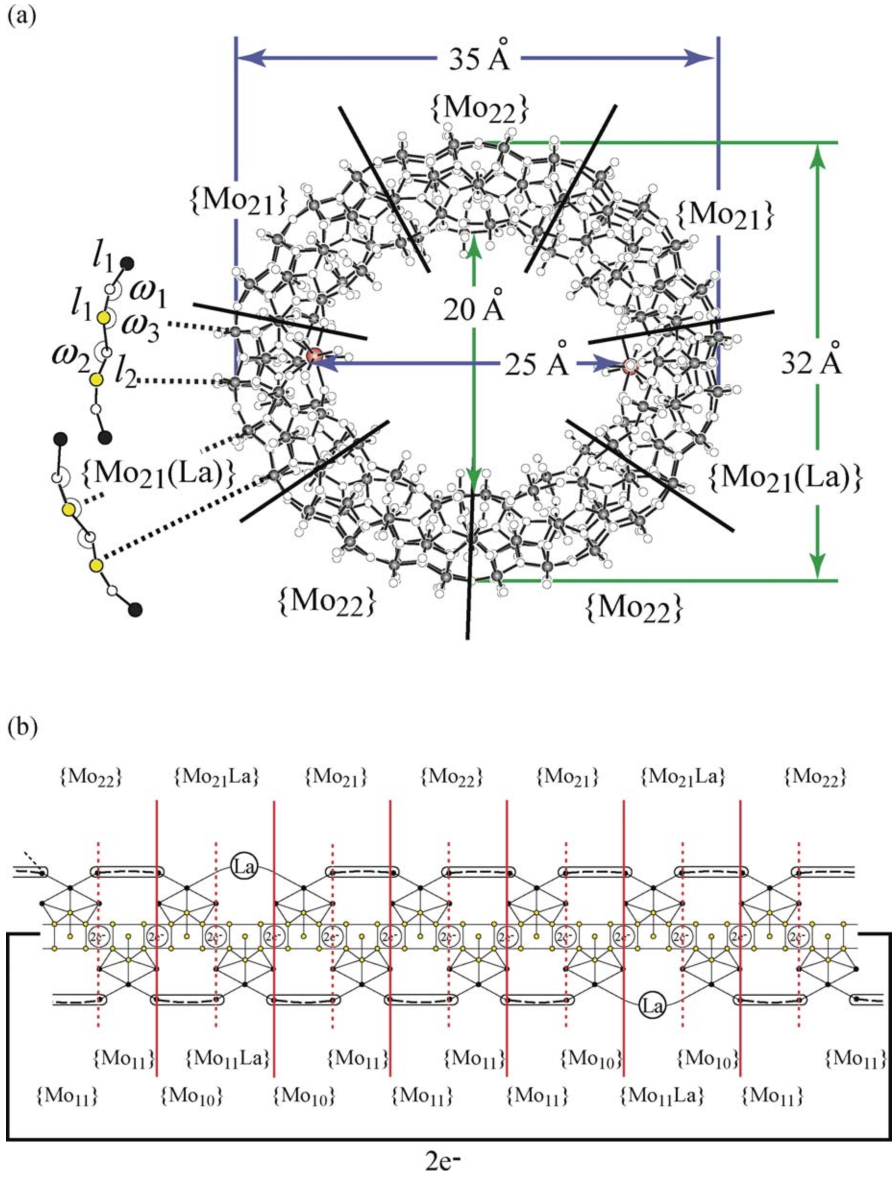

Fig. 2. Structure, building-block sequence, and molecular curvatures of the sub-building-blocks (a) for $[Mo_{28}{}^{V}Mo_{122}{}^{VI}O_{452}H_2(H_2O)_{66}\{La(H_2O)_5\}_2]^{24-}$ (**1a**), and a schematic achievement of **1a** through successive two-electron photoreductions of two-electron reduced building blocks, $2\{Mo_{21}(La)\}$, $2\{Mo_{21}\}$, and $3\{Mo_{22}\}$, which can be divided into $2\{Mo_{11}(La)\}$, $4\{Mo_{10}\}$, and $8\{Mo_{11}\}$ sub-building-blocks (b).

$\mu = 25.41\ \mathrm{cm}^{-1}$, $F(0\,0\,0) = 43{,}792.00$. Crystal size = 0.25 mm × 0.08 mm × 0.04 mm. Crystal was coated with paraffin oil and mounted in a loop. Intensity data were measured on a Rigaku/MSC Saturn CCD diffractometer with the graphite monochromatized Mo Kα radiation ($\lambda = 0.71070$ Å) at 113 K. Data collection proceeded using ω-scan at 0.5° scan and $\chi = 45.0°$ in six runs of $-110.0° < \omega < 70.0°$, $\phi = 0°$; $-110.0° < \omega < 70.0°$, $\phi = 55°$; $-110.0° < \omega < 70.0°$, $\phi = 90°$; $-126.0° < \omega < 54.0°$, $\phi = 0°$; $-126.0° < \omega < 54.0°$, $\phi = 55.0°$; $-126.0° < \omega < 54.0°$, $\phi = 90.0°$. A crystal-to-detector distance was 100.35 mm. The exposure rate was 40.0 s/°. The detector swing angle for the first three runs was −19.98° and for other three runs −35.98°. A total of 1,107,096 reflections ($3.0° < \theta < 27.5°$) was collected of which 47,644 unique reflections ($R_{\mathrm{int}} = 0.1630$) were used. Lorentz polarization factor were applied and a numerical absorption using equivalent reflections was performed with the program ABSCOR (T. Higashi, Program for Absorption Correction. Rigaku Corporation, Tokyo, Japan, 1999). The structure was solved by direct methods (SHELXS97) and refined (3351 parameters) based on a full-matrix least-squares on F^2 by using the CrystalStructure software package (CRYSTALS) to $R = 0.145$ for 36,799 reflections with $I > 3.00\sigma(I)$, $R = 0.251$ for all data: max/min residual electron density 2.97 and -1.92 e Å^{-3}. All the La and Mo atoms were refined anisotropically and all the O atoms isotropically. All the NH_4^+-ammonium N and crystal-water O atoms could not clearly be distinguished using X-ray crystal structure analysis. The site occupancies for disordered atoms of these crystal-water atoms were determined based on refinement of their thermal parameters. The calculation of bond valence sums ($\sum s$) for the oxygen atoms of Mo-O bonds indicated the coordination of 78 aqua ligands (for $\sum s \leq 7$) and 14OH$^-$ ions (for $0.8 \leq \sum s \leq 1.1$) to the anion.

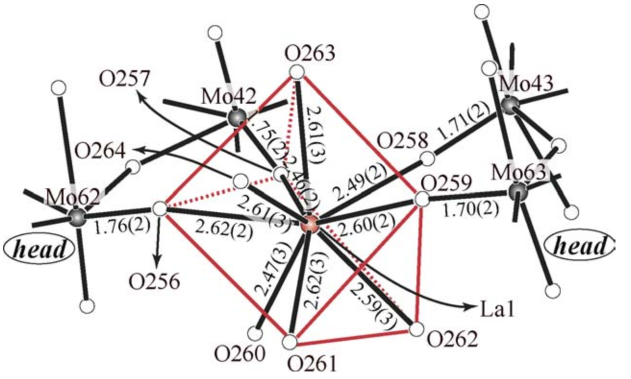

Fig. 3. Environmental geometry of the distorted tricapped-trigonal prism (red color) of LaO_9 site and Mo─O bond distances for **1a**.

3. Results and discussion

Prolonged photolysis of aqueous solutions containing $[Mo_{36}O_{112}(H_2O)_{16}]^{8-}$, $[{}^{i}PrNH_3]^+$, and $LaCl_3$ at pH 1.0 leads to formation of $[{}^{i}PrNH_3]_{24}[Mo_{28}{}^{V}Mo_{122}{}^{VI}O_{452}H_2(H_2O)_{66}\{La(H_2O)_5\}_2]\cdot 156 \pm 5H_2O$ (**1**) crystals. Fig. 2(a) shows nano-ring structure and building-block sequence of the anion (**1a**) for **1**. The structure of **1a** (with a La···La distance of 25.22 Å) is elliptical with an outer and inner ring diameter of approximately 35 and 25 Å, respectively, at its most elongated points, and with outer- and inner-ring diameters of approximately 32 and 20 Å, respectively, at its most compressed points. The ring sequence consists of $2\{Mo_{21}(La)\}$, $2\{Mo_{21}\}$ and $3\{Mo_{22}\}$ building blocks, where $\{Mo_{21}(La)\}$ signifies that a *linker* MoO_6-octahedron in $\{Mo_{22}\}$ is replaced by a LaO_9-distorted tricapped-trigonal prism and $\{Mo_{21}\}$ notifies that a *linker* MoO_6-octahedron in $\{Mo_{22}\}$ is missed for the Mo–O–La linkage between La^{3+} and *head* Mo sites. Fig. 2(b) shows a schematic achievement of **1a** as a 28-electron reduced species through successive two-electron photoreductions of two-electron reduced building blocks, $2\{Mo_{21}(La)\}$, $2\{Mo_{21}\}$, and $3\{Mo_{22}\}$, which could be divided into $2\{Mo_{11}(La)\}$, $4\{Mo_{10}\}$, and $8\{Mo_{11}\}$ sub-building-blocks. **1a** shows the ellipsoidal structure in which two $\{Mo_2\}$-*linkers* associated with the centrosymmetric relationship for the intact $\{Mo_{154}\}$ ring are replaced by two distorted tricapped-trigonal-prismatic La^{3+} ion centers. As shown in Fig. 3, each LaO_9 site coordinated through the replacement of the $\{Mo_2\}$-*linker* in the inner ring consists of four two-coordinate oxygen atoms (1.70–1.76 Å of Mo–O bond-lengths) from $\{Mo_{150}\}$ anions and five aqua oxygen atoms with La–O bond distances of 2.46–2.62 Å. The ellipsoidal structure of **1a** results from the incorporation of largely molecular-curvatured $\{Mo_{21}(La)\}$ building-blocks compared to other building-blocks of $\{Mo_{22}\}$ and $\{Mo_{21}\}$ due to the substitution of the $\{Mo_2\}$-*linker* ($\equiv[Mo(H_2O)O_2(\mu\text{-}O)Mo(H_2O)O_2]^{2+}$) by smaller and more electrophilic $[La(H_2O)_5]^{3+}$ group. By using Mo–O–Mo and O–Mo–O bond angles (ω_1, ω_2 and ω_3) and Mo–O bond distances (l_1 and l_2) for the incomplete double-cubane-type compartments above and below the equator (Figs. 1 and 2), we can estimate the molecular curvature of the incomplete double-cubane-type compartments for each building block [6]. Values of ω_1 and ω_3 for the La^{3+}-coordinating Mo_6O_{23}-related sub-building-block ($\{Mo_{11}(La)\}$) {ω_1 (154–157°, average 156°), ω_2 (137–147°, 142°), ω_3 (153–156°, 155°), l_1 (1.81–1.89, 1.87 Å), and l_2 (2.00–2.14, 2.07 Å)} are smaller than corresponding values {ω_1 (154–160°, 158°), ω_2 (138–144°, 141°), ω_3 (154–159°, 158°), l_1 (1.84–1.94, 1.90 Å), and l_2 (1.98–2.09, 2.05 Å)} for the $\{Mo_2\}$-*linker* coordinating sub-building-blocks ($\{Mo_{11}\}$ and $\{Mo_{10}\}$). If the building block consists of one kind of species, the above values of bond angles and bond-lengths for each sub-building-block enable us to estimate the size of the ring consisting of uniform sub-building-blocks. Since the photoreductive cyclic self-assembly condensation of the largely curvatured $\{Mo_{11}(La)\}$ sub-building-blocks would proceed through missing MoO_6-octahdral *linkers* for the Mo–O–La linkage between La^{3+} and *head* Mo sites, thus, the photoreductive cyclic self-assembled condensation of the resultant $\{Mo_9(La)\}$ species (with almost the same molecular curvature as $\{Mo_{11}(La)\}$) would result in the formation of the 20-electron reduced $\{Mo_{90}(La)_{10}\}$ ring with the ring diameter (D) of approximately 25 Å where all the 10 $\{Mo_2\}$-*linkers* in the inner rings (five for each of above and below the outer ring) are substituted by La^{3+} cations, which corresponds to the $\{Mo_{110}\}$-pentameric ring of $\{Mo_{22}\}$ building-blocks. On the other hand, the photoreductive cyclic self-assembly condensation of the other sub-building-blocks ($\{Mo_{11}\}$ and $\{Mo_{10}\}$) would result in the formation of tetradecameric 28-electron reduced $\{Mo_{154}\}$ (with $D \approx 34$ Å) as discussed previously [6] (Fig. 1). Therefore, the formation of the ellipsoidal shape for **1a** results from the photoreductive condensed self-assembly reactions between the different molecular-curvatured sub-building-blocks according to the sub-building-block sequence of

$\{Mo_{10}\}\{Mo_{11}(La)\}\{Mo_{10}\}\{Mo_{11}\}_4\{Mo_{10}\}\{Mo_{11}(La)\}\{Mo_{10}\}\{Mo_{11}\}_4$

(corresponding to the ring sequence of building blocks

$\{Mo_{21}(La)\}\{Mo_{22}\}_2\{Mo_{21}(La)\}\{Mo_{21}\}\{Mo_{22}\}\{Mo_{21}\}$ (Fig. 2(b)).

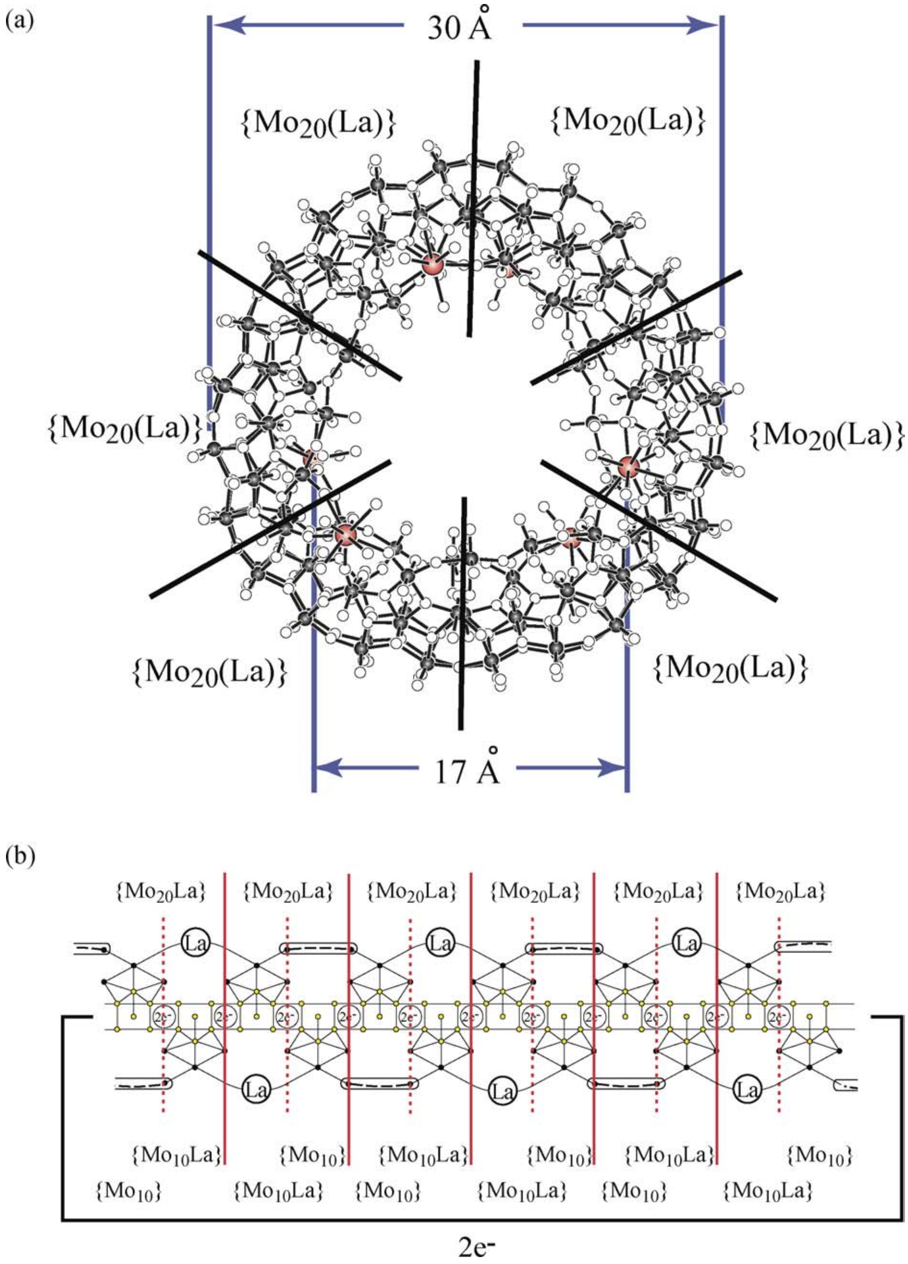

Fig. 4. Structure and building-block sequence (a) of $[Mo_{24}{}^{V}Mo_{96}{}^{VI}O_{366}H_{14}(H_2O)_{48}\{La(H_2O)_5\}_6]^{4-}$ (**2a**), and a schematic achievement of **2a** through successive two-electron photoreductions of two-electron reduced building blocks, $6\{Mo_{20}(La)\}$, which could be divided into $6\{Mo_{10}(La)\}$ and $6\{Mo_{10}\}$ sub-building-blocks (b).

The photochemical manipulation of the ring shape with a combination of two kinds of sub-building-blocks with different molecular curvatures was also revealed for $[Mo_{120}O_{366}H_{14}(H_2O)_{48}\{La(H_2O)_5\}_6]^{4-}$. Prolonged photolysis of acidified solutions (at pH = 1.2 by HCl) containing $[Mo_7O_{24}]^{6-}$, $[p\text{-}CH_3C_6H_4SO_2]^-$, and $LaCl_3$ leads to formation of $[NH_4]_4[Mo_{24}{}^{V}Mo_{96}{}^{VI}O_{366}H_{14}(H_2O)_{48}\{La(H_2O)_5\}_6]\cdot 180 \pm 20H_2O$ (**2**) crystals. Fig. 4(a) shows ring structure and building-block sequence for the anion (**2a**) for **2**. The structure of **2a**, different from the one of **1a**, is of Japanese rice-ball shape with an outer and inner ring diameter of approximately 30 and 17 Å, respectively. The structure of **2a** is the same as $[Mo_{120}\{Pr(H_2O)_5\}_6O_{366}H_{12}(H_2O)_{48}]^{6-}$ which was obtained by heating the aqueous solution containing Na_2MoO_4, $Pr(NO_3)_3$, HCl, and hydrazinium dichloride at 70 °C [9]. All the six LaO_9 sites for **2** are of distorted tricapped-trigonal prism, as well as the case for **1a**. The La···La distances for the La_3 triangle in each of two inner rings are 15.88–16.59 Å and the nearest La···La distances between the two inner rings 12.24–12.88 Å. The building-block sequence consists of $6\{Mo_{20}(La)\}$. Fig. 4(b) shows a schematic achievement of **2a** as a 24-electron reduced species through successive two-electron photoreductions of two-electron reduced building-blocks, $6\{Mo_{20}(La)\}$, which could be divided into $6\{Mo_{10}(La)\}$ and $6\{Mo_{10}\}$ sub-building-blocks as the incomplete double-cubane-type Mo_6O_{23}-related moieties. The molecular curvature of the $\{Mo_{10}(La)\}$ sub-building-block for **2a** is very similar to the one of the La^{3+}-coordinate sub-building-block $\{Mo_{11}(La)\}$ for **1a**, and is larger than that of $\{Mo_{10}\}$which is almost the same as the one of $\{Mo_{10}\}$ or $\{Mo_{11}\}$ for **1a**. Values of ω_1 (154–160°, 157° in average), ω_2 (137–146°, 142°), ω_3 (152–155°, 154°), l_1 (1.86–1.92, 1.90 Å), and l_2 (2.01–2.11, 2.06 Å) for $\{Mo_{10}(La)\}$ predict the formation of the uniform ring as a cyclic decamer of $\{Mo_{10}(La)\}$ sub-building-blocks with $D \approx 25$ Å, if the $\{Mo_{10}(La)\}$sub-building-blocks undergo the self-assembly. Furthermore, a molecular curvature (with $\omega_1 = 157$–161°, 159° in average, $\omega_2 = 137$–140°, 139°, $\omega_3 = 154$–158°, 156°, $l_1 = 1.83$–1.95, 1.88 Å, and $l_2 = 1.98$–2.10, 2.04 Å) for $\{Mo_{10}\}$let us predict the formation of the uniform ring consisting of 14 sub-building-blocks, corresponding to the cyclic heptamer (with $D \approx 34$ Å) of the $\{Mo_{22}\}$ building-blocks. Therefore, the formation of the 24-electron reduced ring of **2a**, as a cyclic hexamer of $\{Mo_{20}(La)\}$ building blocks reflects the successive photoreductive cyclic condensations among $\{Mo_{10}(La)\}$ and $\{Mo_{10}\}$ sub-building-blocks with different molecular curvatures (Fig. 4(b)) according to the sub-building-block sequence of $\underbracket{\{Mo_{10}(La)\}_2\{Mo_{10}\}_2\{Mo_{10}(La)\}_2\{Mo_{10}\}_2\{Mo_{10}(La)\}_2\{Mo_{10}\}_2}$ (corresponding to the sequence of building-blocks $\underbracket{\{Mo_{20}(La)\}_6}$). A large number of incorporation of La^{3+} in **2a** suggests that **2a** may be produced under the high concentration ratio of $[La^{3+}]/[Mo_{36}]$ compared to the case of **1a**. However, **1a** was formed under the condition of $[La^{3+}]/[Mo_{36}] = 2$–7 which is almost the same ratio for the formation of **2a**, implying that the electron donor is also a controlling factor for both the ring shape and the ring size. In conjunction with the fact that both **1** and **2** were formed at almost the same pH level (=1), in addition, the coordination of La^{3+} to the inner rings in **1a** and **2a** is likely to occur through the $La^{3+}\subset\{Mo_{11}\}$ (or $La^{3+}\subset\{Mo_{10}\}$) precursor involved in the photochemical self-assembly rather than the $La^{3+}\subset\{Mo_{154}\}$ precursor after the formation of the $\{Mo_{154}\}$ full-ring.

4. Conclusions

The prolonged photolysis of aqueous solutions containing $[Mo_{36}O_{112}(H_2O)_{16}]^{8-}$, $[{}^{i}PrNH_3]^+$ (or $[p\text{-}CH_3C_6H_4SO_2]^-$), and $LaCl_3$ at pH = 1 leads to the formation of two species of $\{Mo_{150}(La)_2\}$ and $\{Mo_{120}(La)_6\}$ molybdenum-blue nano-rings, which are different in both size and shape. Ln^{3+}-incorporated sub-building-blocks $\{Mo_{10}(Ln)\}$and $\{Mo_{11}(Ln)\}$, which construct $\{Mo_{20}(Ln)\}$ and$\{Mo_{21}(Ln)\}$ building blocks by a combination with$\{Mo_{10}\}$ sub-building-block, exhibit a large molecular curvature with $\omega_1 \approx 157°$ and $\omega_3 \approx 154°$ compared to $\{Mo_{10}\}$and $\{Mo_{11}\}$ with $\omega_1 \approx 158$–159° and $\omega_3 \approx 158°$. Number of the $\{Mo_{10}(Ln)\}$and $\{Mo_{11}(Ln)\}$ sub-building-blocks in the building-block sequence for the ring is important for both shape and size of the nano-rings photochemically derived from the $\{Mo_{154}\}$ full-ring, which is governed by the manipulation of Ln^{3+} (with a variety of ionic radius) and electron donors. Since heavy Ln^{3+} cations (with small ionic radii) such as Yb^{3+} and Er^{3+} will lead to larger molecular curvature of the $\{Mo_{10}(Ln)\}$and $\{Mo_{11}(Ln)\}$ sub-building-blocks, it is possible to expect new possibilities for further functionalization (based on the magnetic and electronic intramolecular interactions) as well as the shape of the nano-rings by using a combination with different molecular-curvatured sub-building-blocks. The photochemistry of the molybdenum blues is not only suitable for the mechanistic investigation of the self-assembly reaction of the molybdenum blues but also promising for the molecular design of the nano-rings in the nanostructure landscape.

5. Supporting information

X-ray crystallographic files for **1** and **2** in CIF format can be ordered from Fachinformationszentrum Karlsruhe, Hermann-von-Helmholtz-Platz 1, 76344 Eggenstein-Leopoldshafen, Germany, http://icsd.fiz-karlsruhe.de by quoting the depository numbers CSD-414658 (**1**) and CSD-414659 (**2**).

References

[1] T. Yamase, J. Chem. Soc., Dalton Trans. (1991) 3055–3063.

[2] A. Müller, E. Krickemeyer, H. Bögge, M. Schmidtmann, C. Beugholt, S.K. Das, F. Peters, Chem. Eur. J. 5 (1999) 1496–1502.

[3] L. Cronin, C. Beugholt, A. Müller, J. Mol. Struct. (Theochem.) 500 (2000) 181–193.
[4] A. Müller, P. Kögerler, A.W.M. Dress, Coord. Chem. Rev. 222 (2001) 193–218.
[5] P. Kögerler, A. Müller, in: T. Yamase, M.T. Pope (Eds.), Polyoxometalate chemistry for nano-composite design, KluwerAcademic/Plenum Pubs, New York, 2002, pp. 1–15.
[6] T. Yamase, P. Prokop, Angew. Chem. Int. Ed. Engl. 41 (2002) 466–469.
[7] T. Yamase, P. Prokop, Y. Arai, J. Mol. Struct. 656 (2003) 107–117.
[8] B. Krebs, S. Stiller, K.H. Tytko, J. Mehmke, Eur. J. Solid State Inorg. Chem. t.28 (1991) 883–903.
[9] A. Müller, C. Beugholt, H. Bögge, M. Schmidtmann, Chem. Commun. (2001) 3112–3113.
[10] L. Cronin, C. Beugholt, E. Krickemeyer, M. Schmidtmann, H. Bögge, P. Kögerler, T. Kim, K. Luong, A. Müller, Angew. Chem. Int. Ed. Engl. 41 (2002) 466–469.